Increasing the Milling Accuracy for Industrial Robots Using a Piezo-Actuated High-Dynamic Micro Manipulator

Sörnmo, Olof; Olofsson, Björn; Schneider, Ulrich; Robertsson, Anders; Johansson, Rolf

Published in:
2012 IEEE/ASME International Conference on Advanced Intelligent Mechatronics (AIM)

DOI:
10.1109/AIM.2012.6265942

2012

The 2012 IEEE/ASME International Conference on
Advanced Intelligent Mechatronics
July 11-14, 2012, Kaohsiung, Taiwan

Increasing the Milling Accuracy for Industrial Robots Using a Piezo-Actuated High-Dynamic Micro Manipulator

Olof Sörnmo, Björn Olofsson, Ulrich Schneider, Anders Robertsson and Rolf Johansson

***Abstract*— The strong process forces arising during high-speed machining operations, combined with the limited stiffness of industrial robots, have hampered the usage of industrial robots in high-end milling tasks. However, since such manipulators may offer flexible and cost-effective machining solutions, a three-dimensional piezo-actuated compensation mechanism, which aims to compensate for the positioning errors of the robot, has earlier been developed. A prototype model-based control scheme for position control of the mechanism, utilizing LQG control, has been proposed. The main contribution of this paper is an experimental verification of the benefit of utilizing the online compensation scheme. We show that the milling accuracy achieved with the proposed compensation mechanism is increased up to three times compared to the uncompensated case.**

I. Introduction

Because of the increased demands on efficiency and flexibility in industrial production over the past decades, the need for automated and high-accuracy machining operations has increased. In this context, usage of industrial robots is an appealing solution based on its flexibility in terms of reconfiguration possibilities, versatility and its relatively low investment cost, compared to the cost of a machine-tool. However, due to the limited stiffness and position-accuracy of industrial robots, machining operations are not straightforward to perform [1], [2].

Within the EU/FP7 project COMET [3], the aim is to increase the accuracy of machining solutions for industrial robots. In particular, milling solutions with an accuracy below 50 μm are developed. For high-accuracy milling, a three-dimensional piezo-actuated compensation mechanism has already been developed [4], [5]. The mechanism is to compensate for the remaining position errors of the robot, which the robot *per se* is unable to compensate for due to its limited structural bandwidth compared to its eigenfrequencies. In the proposed setup, the spindle holding the milling tool is attached to the compensation mechanism and the robot is holding the workpiece, see Fig. 1. We developed a model-based control scheme, which was tested on the compensation mechanism with satisfactory results [6].

The main contribution of this paper is an experimental verification of the proposed control scheme for machining with industrial robots, presenting results from milling tasks in aluminium. The experimental verification contrasts the milling accuracy using the compensation mechanism to the standard uncompensated case.

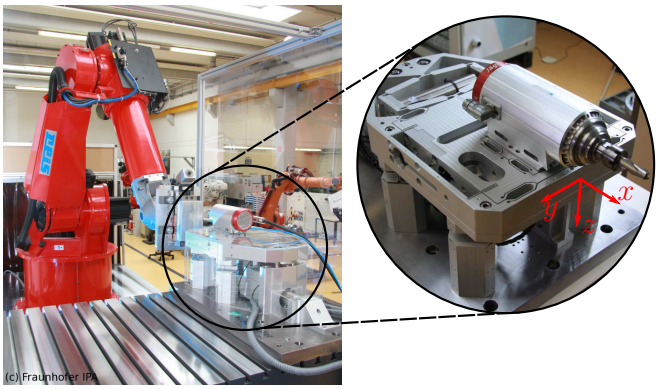

Fig. 1. The experimental setup for real-time compensation of positioning errors during machining operations, where the robot holds the workpiece and the milling spindle is attached to the micro manipulator. A close-up of the micro manipulator, as seen from the opposite side, is displayed to the right in the figure.

The advantages of utilizing an additional manipulator together with a robot in a closed kinematic chain, has been investigated by Sharon *et al.*, see, *e.g.*, [7]. It was shown that the bandwidth of the endpoint position control loop was increased. The concepts of macro and micro manipulator were introduced to describe the robot and the additional compensation mechanism, respectively. These terms will be adopted in this paper. Note, however, that the micro manipulator in the proposed experimental setup is not attached to the robot.

Piezo-actuated mechanisms based on flexure-elements have been proposed for micro and nano manipulation, see, *e.g.*, [8], [9]. Although the compensation mechanism proposed in this paper has a similar mechanical design, there are significant differences. Previous designs were designed for compensation in micro and nano manipulation, whereas the micro manipulator discussed in this paper is designed for machining processes with industrial robots, where strong process forces are required.

In [10], a control scheme for task space control of industrial manipulators, with a hierarchical structure similar to the one utilized for control of the micro manipulator discussed in this paper, is presented. However, the control of the micro manipulator in this paper is performed directly in task space, due to the decoupled nature of the actuation mechanism.

O. Sörnmo, B. Olofsson, A. Robertsson and R. Johansson are with the Department of Automatic Control, LTH, Lund University, SE–221 00 Lund, Sweden. E–mail: Olof.Sornmo@control.lth.se.

U. Schneider is with Fraunhofer Institute for Manufacturing and Engineering, Nobelstraße 12, D–70569 Stuttgart, Germany.

The research leading to these results has received funding from the European Union's seventh framework program (FP7/2007-2013) under grant agreement #258769 COMET.

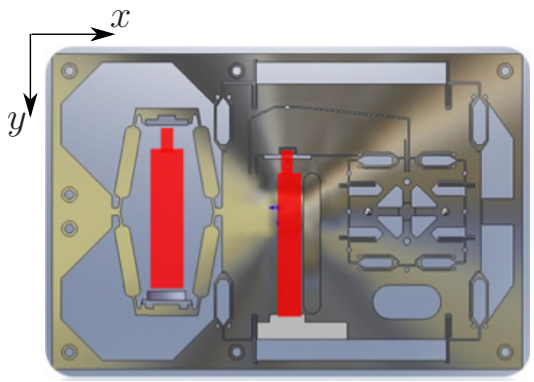

Fig. 2. Actuation principle for the x- and y-axes of the micro manipulator. The piezo actuators are marked by red color in the drawing [4].

This paper is organized as follows. The design of the micro manipulator and the earlier proposed scheme for position control are briefly reviewed in Sec. II. Further, the interaction of the micro manipulator with the robot controller is discussed. Section III defines the setup used for experimental evaluation of the micro manipulator. The experimental results from milling tasks are presented in Sec. IV. A subsequent evaluation is presented in Sec. V, followed by a discussion in Sec. VI. Finally, conclusions and aspects on future work are given in Sec. VII.

II. Micro manipulator design and control

A. Micro manipulator design

The design of the micro manipulator is such that motion of the machining spindle is possible in all three Cartesian directions. Referring to Fig. 1, the axes are hereafter called x, y, and z, respectively. The mechanism is actuated by piezo-actuators, whose movements are transferred to a corresponding translational movement of the spindle *via* a flexure mechanism (Fig. 2). For further details regarding the mechanical design, the reader is referred to [4].

The gear ratio in each of the axes from motor to arm side is approximately five, which results in a maximum compensation range of about 0.5 mm in each direction. The micro manipulator is equipped with strain gauges attached to the piezo-actuators as well as capacitive sensors, which measure the Cartesian position of the spindle.

B. Control architecture

The proposed control architecture for the industrial robot and the micro manipulator is displayed in Fig. 3. It consists of three main components; the robot controller, a tracking system, and the micro manipulator controller.

1) Robot controller: The industrial robot is controlled by a conventional robot controller. The path to be tracked is planned offline and any deviation from this path during the milling process is detected by an online tracking system and subsequently compensated by the micro manipulator.

2) Tracking system and path deviation detection: An optical system is utilized for tracking of the workpiece. The workpiece is, in the proposed setup, held by the robot. As a prototype tracking system, laser-based sensors are utilized for tracking of the position of the workpiece. However, any optical tracking system with sufficient resolution and sample rate can be utilized. Sufficient resolution in this context is determined by the desired milling accuracy.

The position of the workpiece, as measured by the tracking system, is compared to the nominal position calculated in the robot controller. Deviations from the nominal path are fed to the micro manipulator controller.

3) Micro manipulator controller: The position control of the compensation mechanism is handled by the micro manipulator controller. Based on the reference value calculated by the tracking system, the controller positions the micro manipulator, and consequently the attached machining tool. The micro manipulator control scheme is discussed next.

C. Control scheme for position control

In [6], we proposed a control scheme for position control of the micro manipulator. The control scheme must handle both the nonlinear effects in the piezo-actuators and the inherent resonant character of the mechanical construction. In the control scheme, each of the Cartesian directions of the construction was considered separately and a controller was designed for each axis. The control structure is depicted in Fig. 3. As a prototype controller, an inner high-gain PID controller loop, with feedback from the strain gauge sensor, was proposed. The transfer function of the PID controller is given by

$$G_C(s) = K_p + \frac{K_i}{s} + \frac{sK_d}{1 + sK_d/N} \tag{1}$$

where K_p, K_i, and K_d are controller parameters and N determines the cut-off frequency for the low-pass filter in the D-part. Furthermore, the I-part is accompanied by an anti-windup scheme.

1) Model identification and control: With the inner control loop closed, identification of the linear dynamics of the micro manipulator was performed using system identification methods [11]. Thereby, discrete-time state-space models, parametrized in the matrices $\{\Phi, \Gamma, C, D\}$, of the format

$$\begin{cases} x_{k+1} = \Phi x_k + \Gamma u_k + v_k \\ y_k = C x_k + D u_k + e_k \end{cases} \tag{2}$$

where $u_k \in \mathbb{R}^m$ is the input; $x_k \in \mathbb{R}^n$ the state vector; $y_k \in \mathbb{R}^p$ the output; v_k and e_k noise sequences, were considered. The subspace-based identification methods MOESP [12] and N4SID [13] were found to result in models with superior fit to experimental data. In particular, the natural eigenfrequencies of the micro manipulator were identified with higher accuracy with subspace-methods compared to identification of ARMAX models [11].

Based on the identified models, a state-feedback control scheme, including Kalman filters for estimating the states not available for measurements, was developed and subsequently

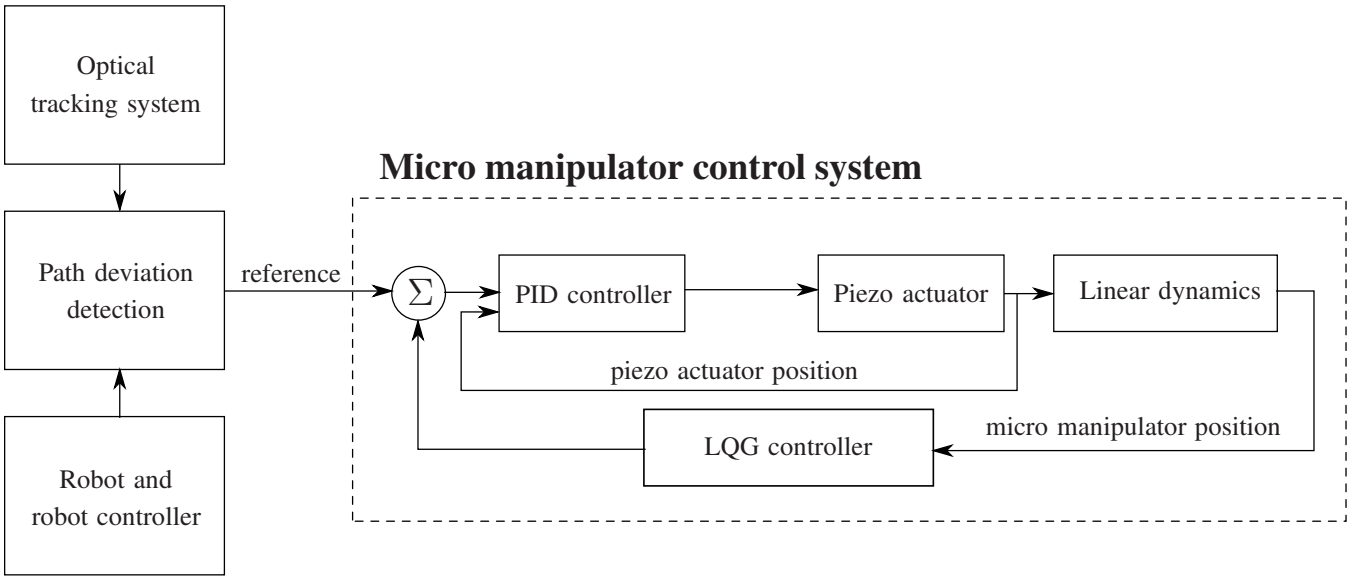

Fig. 3. Control architecture for online compensation of position errors during milling operations with industrial robots. The micro manipulator control scheme positions the machining tool based on the reference value calculated as the deviation of the robot from the nominal path.

implemented and tested in experimental evaluations. The gain vector of the state feedback was determined by linear-quadratic (LQ) optimal control [14]. For more details on model identification and the control scheme for the micro manipulator, the reader is referred to [6].

2) Outlier detection: In order to make the measurements from the laser-based tracking system more robust, an outlier detection scheme is utilized in the micro manipulator controller. The outliers in the current setup are due to aluminium chips emitted from the milling process, crossing the laser beam and resulting in a temporary deviation from the correct measurement. Even though the outliers are infrequent, they have to be handled actively. Therefore, an online outlier detection scheme with prediction of measurements [15], was implemented in the controller.

III. Experimental setup

The experimental evaluation was performed using a REIS industrial robot of model RV40 [16]. The spindle was attached to the micro manipulator and the robot held the workpiece, which in this case was a block of aluminium (AlMg3,5). The setup is such that both face milling and peripheral milling, also referred to as radial milling, can be performed, see Fig. 1.

A. Interface and sensors

The micro manipulator was interfaced with a dSPACE controller board of model DS1103 [17], where the developed controllers were executed at a sampling frequency of 10 kHz. The controllers were implemented in MATLAB Simulink and C–code was generated by the Real-Time Workshop toolbox [18]. The compiled C–code was then executed in the dSPACE system.

To the purpose of measuring the deflections of the robot in the milling direction, *i.e.*, the deflections which were to be compensated by the micro manipulator, a Keyence laser sensor of model LK-G87 [19], with a resolution of 0.2 μm was used as a prototype tracking system.

B. Compensated and uncompensated milling

In order to illustrate the benefit of the micro manipulator, the milling experiments were performed both in a setting where compensation with the micro manipulator was utilized and in a setting with the spindle rigidly attached to a fixed base. In the latter setup, no compensation is performed. The two experimental settings are displayed in Fig. 4.

In the experiments without compensation, the robot configuration was mirrored, with respect to the center plane of the robot, compared to the configuration chosen in the experiments with compensation. Consequently, the compliance properties of the robot in the two configurations are equivalent. Mirroring is important in order to make the compensated and uncompensated milling results comparable.

IV. Experimental results

With the experimental setup described in Sec. III, milling in aluminium was performed. The robot can be reconfigured such that milling can be executed in all three directions of the micro manipulator. Results obtained during face milling in the x-direction and peripheral milling in the y- and z-directions of the micro manipulator are presented. The experiments were performed with a material feed-rate of 7.5 mm/s, a spindle speed of 28 000 rpm and a depth of cut of 1 mm in the face millings and 1×10 mm in the peripheral millings.

A. Milling experiments with compensation

1) X-direction: In the first setting, face milling is performed, where the surface orthogonal to the x-axis of the micro manipulator is to be machined. Consequently, the micro

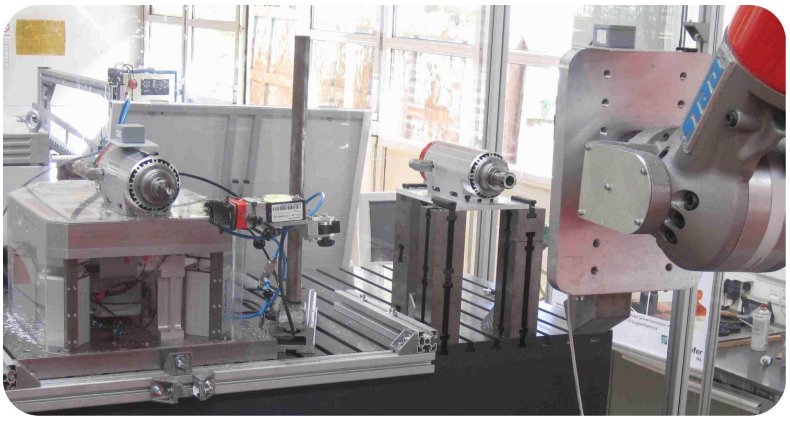

Fig. 4. Experimental setup for evaluation of the effectiveness of the proposed micro manipulator, which is seen to the left. The machining spindle to the right is rigidly attached to the base. This setup is utilized for milling experiments without compensation.

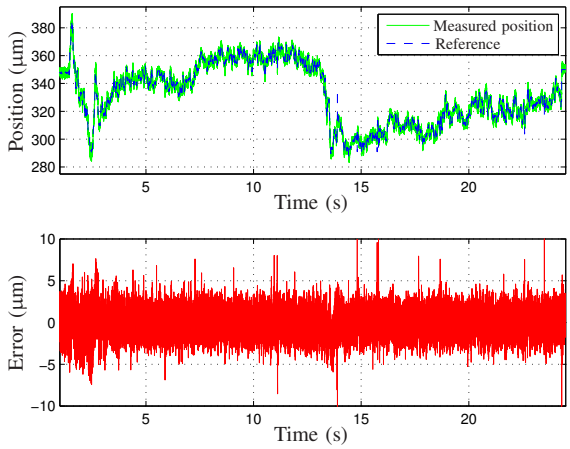

Fig. 5. Reference and position of the micro manipulator during milling experiment in the x-direction (upper panel) and corresponding control error (lower panel).

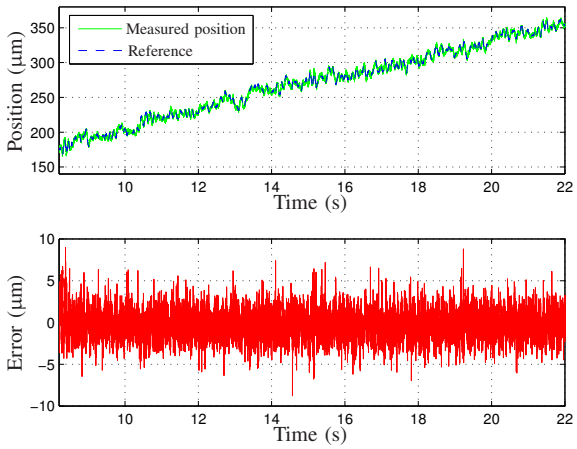

Fig. 6. Reference and position of the micro manipulator during milling experiment in the y-direction (upper panel) and corresponding control error (lower panel).

manipulator is controlled in this direction. The result of the milling experiment is displayed in Fig. 5. The control error is defined as the difference between the reference value to the micro manipulator control system and the measurement from the capacitive sensor in the x-direction of the micro manipulator.

2) Y-direction: The milling accuracy has further been tested in a peripheral milling, where the compensation was performed in the y-axis of the micro manipulator. It should be noted that this milling task is different from the face milling presented in the previous paragraph, in the sense that the process forces affect the robot differently.

Furthermore, the experiment is designed such that the robot, on purpose, is not moving perpendicularly to the compensation direction. This situation can be considered as a result of a poorly calibrated workpiece or industrial robot. By utilizing the micro manipulator, this effect can be compensated since the movement of the robot is tracked in real-time.

The result of the milling experiment is displayed in Fig. 6. The control error displayed is defined analogously to the case with face milling in the x-direction of the micro manipulator.

3) Z-direction: The third experiment was a peripheral milling along the z-axis of the micro manipulator. The control performance of the micro manipulator in the milling experiment is displayed in Fig. 7.

B. Milling experiments without compensation

The same milling experiments described and presented in the previous subsection were repeated, but with the machining spindle rigidly attached—*i.e.*, no online compensation was active. The results of the experiments will be evaluated in the subsequent section.

V. Experimental Evaluation

A. Coherence spectra

An important aspect to consider in the control scheme is if the nonlinear effects in the piezo-actuators influence the

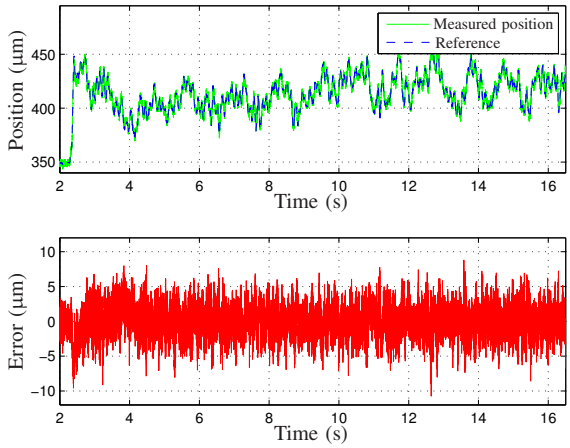

Fig. 7. Reference and position of the micro manipulator during milling experiment in the z-direction (upper panel) and corresponding control error (lower panel).

frequency characteristics of the micro manipulator. For that purpose, the quadratic coherence spectrum [11], *i.e.*,

$$\gamma_{uy}(\omega) = \frac{|S_{uy}(i\omega)|^2}{S_{uu}(i\omega)S_{yy}(i\omega)}, \tag{3}$$

where $S_{uy}(i\omega)$ is the power cross-spectrum between input u and output y, $S_{uu}(i\omega)$ and $S_{yy}(i\omega)$ are the autospectra for u and y, respectively, is investigated. The coherence spectra for the x-, y-, and z-directions of the micro manipulator are displayed in Fig. 8.

It is observed that the relation between input and output in the x- and z-directions appears to be linear. In the corresponding spectrum for the y-direction, the coherence is clearly below one in the frequency range about 65 Hz, which is the result of a poorly damped zero in the system. However, since this frequency is above the bandwidth of the controller, the influence of the zero is small.

B. Frequency analysis of control error

From a control theory point of view, the results obtained from the milling experiments should be evaluated by examining if there is more information available in the control error—*i.e.*, separating the noise in the measurements from the possibly available information, which should be acted upon.

To this purpose, ARMA-models as well as frequency spectra of the control errors are estimated. The latter are estimated using Welch's method [11]. The estimated power spectral densities (PSD) for the control error in the performed milling experiments are displayed in Fig. 9. The spectra are further discussed in Sec. VI.

C. Measurement of milling profiles

Since the main objective of the milling experiments is to achieve a high accuracy of the machined surface on the workpiece, a Mahr measurement device of model M400 SD26 [20] was utilized to measure the surface roughness of

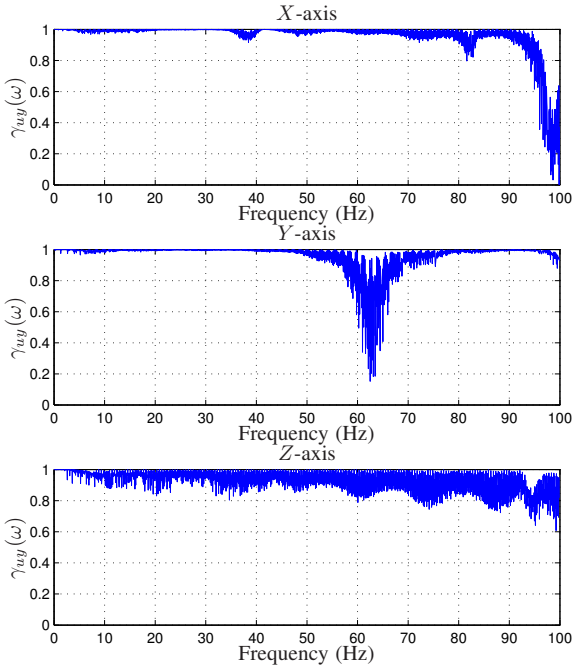

Fig. 8. Estimated coherence spectra with the inner PID control loop active, in the x-, y-, and z-directions of the micro manipulator.

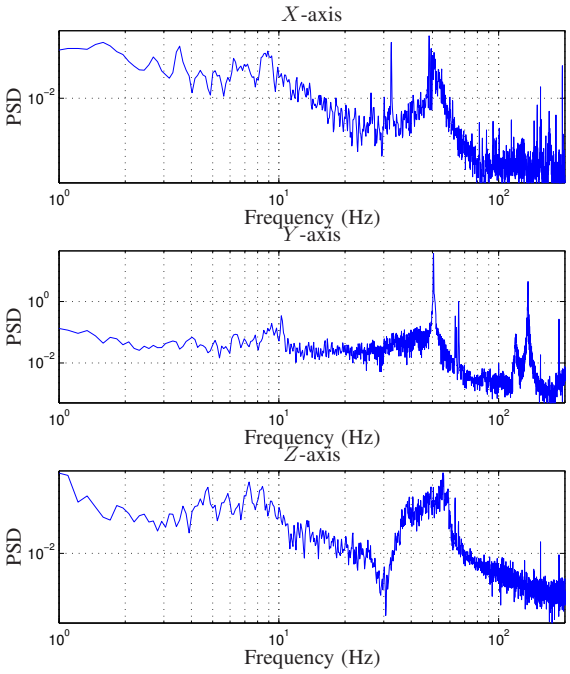

Fig. 9. Estimated power spectral densities for the control error in all directions of the micro manipulator.

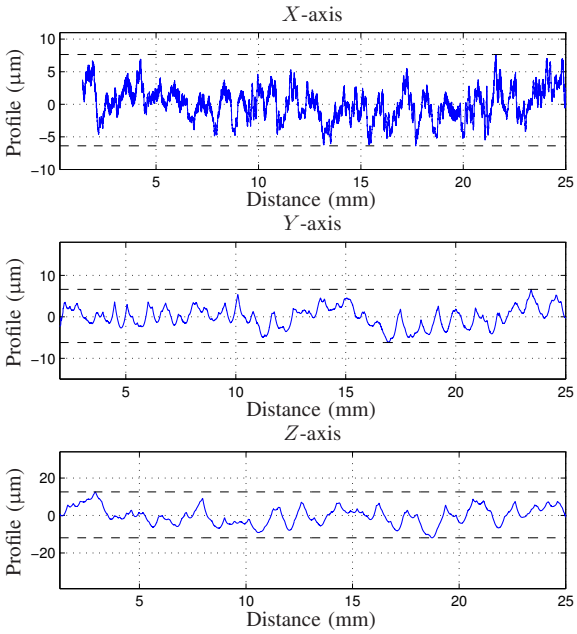

Fig. 10. Profiles after face milling in x-direction and peripheral milling in y- and z-directions of the micro manipulator. In all experiments online compensation with the micro manipulator was utilized.

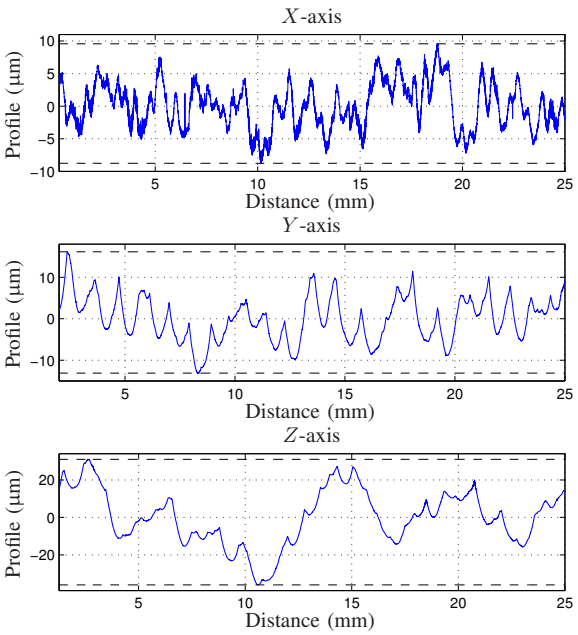

Fig. 11. Profiles after uncompensated milling in the x-, y-, and z-directions of the micro manipulator, respectively.

the obtained profiles. The measurement device is calibrated such that it has a measurement accuracy below 1 μm.

1) Milling with compensation: The results of the surface roughness measurements, for the three milling experiments with online compensation, are displayed in Fig. 10. The measured profiles indicate that the milling accuracy in the x- and y-directions are within ± 7 μm and that the error of the measured milling profile is within approximately ± 12 μm in the z-direction of the micro manipulator. Furthermore, it is noted that the measured profiles correspond well to the measurements from the capacitive sensors attached to the micro manipulator, which are used for feedback. This correspondence provides experimental confirmation that the measured position of the compensation mechanism agrees with the actual position of the milling tool. Photos of the milled surfaces for the experiments in the x- and y-directions are provided in Figs. 12–13.

2) Milling without compensation: The resulting surface roughness of the profiles from the uncompensated milling experiments, as measured by the Mahr device, is displayed in Fig. 11. To evaluate the quality of the measured profiles from the experiments with online compensation compared to the profiles obtained in milling without compensation, both the maximum error e_m and the standard deviation σ_e of the profiles are calculated. Table I shows the maximum errors of the profiles, calculated as the minimum value subtracted from the maximum value, and the standard deviations from the nominal profiles.

TABLE I

MAXIMUM ERROR e_m AND STANDARD DEVIATION σ_e OF MILLING PROFILE

Axis	e_m compensated (μm)	e_m uncompensated (μm)	Ratio
x	14.0	18.3	1.3
y	12.8	29.3	2.3
z	24.5	67.0	2.7
Axis	**σ_e compensated (μm)**	**σ_e uncompensated (μm)**	**Ratio**
x	2.8	7.6	2.7
y	2.5	5.6	2.2
z	4.7	14.9	3.2

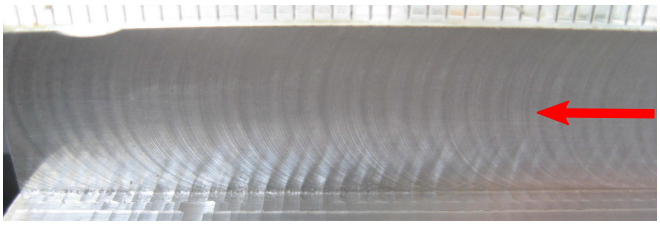

Fig. 12. Workpiece after face milling on the surface indicated by the red arrow, with compensation in the x-direction of the micro manipulator.

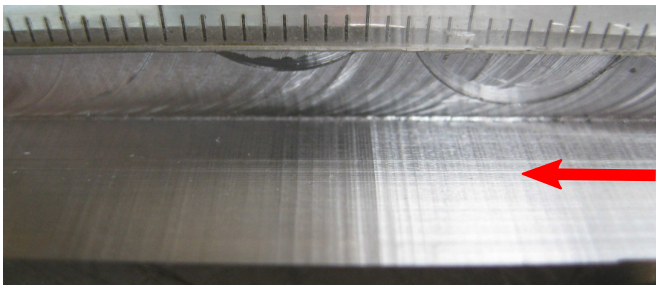

Fig. 13. Workpiece after peripheral milling on the surface indicated by the red arrow, with compensation in the y-direction of the micro manipulator.

VI. Discussion

Given the results in Table I, it is evident that online compensation with the micro manipulator has improved the milling accuracy significantly compared to the uncompensated case. From the experimental evaluation, it can be concluded that the control error in the micro manipulator control scheme is below ± 12 µm in all axes, which is well below the desired accuracy of 50 µm.

Several conclusions can be drawn from frequency analysis of the control error. All frequency spectra of the control errors in Fig. 9 exhibit peaks at approximately 10 Hz and at 50 Hz. The latter is a disturbance from the power network system. The former relates to the eigenfrequencies of the industrial robot in the corresponding Cartesian directions. This is experimentally confirmed by modal analysis of the REIS RV40 robot [21]. However, while the peaks are visible, they are not prominent. This suggests that the micro manipulator controller can attenuate the most important disturbance during the milling—*i.e.*, the natural eigenfrequencies of the robot.

The achievable bandwidth of the position controller for the industrial robot is limited by the natural eigenfrequencies of the mechanical construction and the non-colocated sensing and actuation—*i.e.*, joint-based actuation and task space measurements of the position of the workpiece [22]. The advantage of utilizing the proposed micro manipulator is the significantly increased bandwidth of the end-effector position control, which is the result of the colocation of the actuation—with the micro manipulator—and the task space sensors [7]. In the current experimental setup, the bandwidth of the micro manipulator is 3–4 times higher than that of the industrial robot.

Further, the influence of the mechanical design of the micro manipulator on the milling performance is visible in the spectra of Fig. 9. The zero in the z-direction of the micro manipulator at 30 Hz is clearly visible in the corresponding frequency spectrum. Likewise, one of the natural eigenfrequencies of the micro manipulator in the x-axis at 32 Hz is visible. The bandwidth of the closed-loop position controller for the micro manipulator is consequently limited by the mechanical design.

VII. Conclusions and future work

This paper has investigated the milling accuracy of industrial robots by utilizing a high-dynamic, piezo-actuated, micro manipulator for demanding machining processes. It was shown in an experimental verification that the proposed method offers significantly higher accuracy in terms of surface roughness, compared to the standard method for milling without online compensation.

Future work will focus on increasing the milling accuracy even further, by optimizing the mechanical design of the micro manipulator with the aim of increasing the bandwidth of the closed-loop control system. Also, multi-dimensional milling experiments will be performed, where compensation with the micro manipulator will be executed in several directions simultaneously.

References

[1] H. Zhang, J. Wang, G. Zhang, Z. Gan, Z. Pan, H. Cui, and Z. Zhu, "Machining with flexible manipulator: Toward improving robotic machining performance," in *Proc. IEEE/ASME Int. Conf. Adv. Intelligent Mechatronics*, Monterey, California, USA, July 2005, pp. 1127–1132.

[2] E. Abele, J. Bauer, T. Hemker, R. Laurischkat, H. Meier, S. Reese, and O. von Stryk, "Comparison and validation of implementations of a flexible joint multibody dynamics system model for an industrial robot," *CIRP J. Manufacturing Science and Technology*, vol. 4, no. 1, pp. 38–43, 2011.

[3] COMET, 2011, EU/FP7-project: *Plug-and-produce COmponents and METhods for adaptive control of industrial robots enabling cost effective, high precision manufacturing in factories of the future*, Available: http://www.cometproject.eu, Jan. 10, 2012.

[4] A. Puzik, A. Pott, C. Meyer, and A. Verl, "Industrial robots for machining processes in combination with an additional actuation mechanism for error compensation," in *7th Int. Conf. on Manufacturing Research (ICMR)*, University of Warwick, UK, September 2009.

[5] A. Puzik, C. Meyer, and A. Verl, "Results of robot machining with additional 3D-piezo-actuation-mechanism for error compensation," in *7th CIRP Int. Conf., Intelligent Computation in Manufacturing Eng.: Innovative and Cognitive Production Technology and Systems*, Capri, Italy, June 2010.

[6] B. Olofsson, O. Sörnmo, U. Schneider, A. Robertsson, A. Puzik, and R. Johansson, "Modeling and control of a piezo-actuated high-dynamic compensation mechanism for industrial robots," in *Proc. IEEE/RSJ Int. Conf. on Intelligent Robots and Systems*, San Francisco, California, USA, September 2011, pp. 4704–4709.

[7] A. Sharon, N. Hogan, and D. E. Hardt, "The macro/micro manipulator: An improved architecture for robot control," *Robotics & Computer-Integrated Manufacturing*, vol. 10, no. 3, pp. 209–222, 1993.

[8] Y. Li and Q. Xu, "A totally decoupled piezo-driven XYZ flexure parallel micropositioning stage for micro/nanomanipulation," *IEEE Trans. Automation Science and Eng.*, vol. 8, no. 20, pp. 265–279, 2011.

[9] H. C. Liaw and B. Shirinzadeh, "Constrained motion tracking control of piezo-actuated flexure-based four-bar mechanisms for micro/nano manipulation," *IEEE Trans. Automation Science and Eng.*, vol. 7, no. 3, pp. 699–705, July 2010.

[10] N. D. Vuong, M. H. Ang Jr., T. M. Lim, and S. Y. Lim, "Multi-rate operational space control of compliant motion in robotic manipulators," in *Proc. IEEE Int. Conf. Systems, Man and Cybernetics*, San Antonio, Texas, USA, October 2009, pp. 3175–3180.

[11] R. Johansson, *System Modeling and Identification*. Englewood Cliffs, New Jersey: Prentice Hall, 1993.

[12] M. Verhaegen and P. Dewilde, "Subspace model identification—The output-error state-space model identification class of algorithms," *Int. J. Control*, vol. 56, pp. 1187–1210, 1992.

[13] P. van Overschee and B. De Moor, "N4SID: Subspace algorithms for the identification of combined deterministic-stochastic systems," *Automatica*, vol. 30, no. 1, pp. 75–93, 1994.

[14] K. J. Åström and B. Wittenmark, *Computer-Controlled Systems*. Englewood Cliffs, New Jersey: Prentice Hall, 1997.

[15] P. H. Menold, R. K. Pearson, and F. Allgöwer, "Online outlier detection and removal," in *Proc. of the 7th Mediterranean Conf. on Control and Automation (MED99)*, June 1999, pp. 1110–1133.

[16] *Reis RV40 Fact Sheet*. Obernburg, Germany: Reis GmbH, 2011.

[17] *DS1103 PPC Controller Board—Hardware Installation and Configuration*. Paderborn, Germany: dSPACE GmbH, 2007.

[18] *Real-Time Workshop 7: Users's Guide*. Natick, Massachusetts: The MathWorks, Inc., 1994–2010.

[19] *LK-G Series User Manual*. Osaka, Japan: Keyence Corp., 2006.

[20] *MarSurf M 400 Flyer*. Göttingen, Germany: Mahr GmbH, 2011.

[21] U. Schneider, "Regelung einer 3D-Ausgleichsaktorik für Fräsanwendungen mit Industrierobotern," Diploma Thesis, Fraunhofer Institute for Manufacturing and Engineering, Stuttgart, Germany, March 2010.

[22] E. Fasse and N. Hogan, "Control of physical contact and dynamic interaction," in *Proc. 7th Int. Symp. Robotics Research*, Munich, Germany, October 1995, pp. 28–38.